International Immunopharmacology 75 (2019) 105836

Contents lists available at ScienceDirect

International Immunopharmacology

journal homepage: www.elsevier.com/locate/intimp

TRPM2 channel regulates cytokines production in astrocytes and aggravates brain disorder during lipopolysaccharide-induced endotoxin sepsis

Tao Zhu[a], Yisha Zhao[b,c], Hui Hu[b,d], Qianqian Zheng[b,e], Xiaoying Luo[b], Yinjie Ling[b,f], Yingchao Ying[b], Zheng Shen[b], Peifang Jiang[b,*], Qiang Shu[b,*]

[a] Department of Critical Care Medicine, Sir Run Run Shaw Hospital, School of Medicine, Zhejiang University, Hangzhou, Zhejiang, China
[b] Department of Neurology, Zhejiang Key Laboratory for Diagnosis and Treatment of Neonatal Diseases, Children's Hospital, School of Medicine, Zhejiang University, Hangzhou, Zhejiang, China
[c] Department of Pediatrics, Wenling Maternal and Child Health Care Hospital, Wenling, Zhejiang, China
[d] Department of Pediatrics, Lishui Maternal and Child Health Care Hospital, Lishui, Zhejiang, China
[e] Department of Peditrica, Sanmen People's Hospital, Sanmen, Zhejiang, China
[f] Department of Peditrica, first people's hospital of Huzhou, Huzhou, Zhejiang, China

ARTICLE INFO

Keywords:
TRPM2
Sepsis
Astrocyte
Inflammatory mediators
Apoptosis

ABSTRACT

Sepsis is one of the most significant challenges in intensive care units, which is associated with increased morbidity and mortality. Sepsis-associated encephalopathy (SAE) is a severe complication which can cause death and serious disabilities. Calcium signaling in astrocyte is essential for cellular activation and the potential resolution of infection or inflammation in SAE patients. The transient receptor potential melastatin 2 (TRPM2) channel has been identified as a unique fusion of a Ca^{2+}-permeable nonselective cation channel, which plays an important role in inflammation and immune response. Because of its role as an oxidative stress sensor in astrocytes, we investigated the function of TRPM2 in inflammation mediators (interleukin (IL)-1β, IL-6 and tumor necrosis factor (TNF)-α) release, Bcl-2/E1B-19 K-interacting protein 3 (BNIP3), apoptosis inducing factor (AIF) and Endonuclease G (Endo G) expression. We showed that TRPM2-KO mice, when intraperitoneally (i.p) injected with LPS, exhibited better neurologic assessment scores and decreased inflammatory injury in hippocampal neurons compared with wild-type (WT) mice. The absence of TRPM2 triggered less production of inflammatory mediators (IL-1β, IL-6, TNF-α) and decreased apoptosis related proteins (BNIP3, AIF, Endo G) expressions in response to LPS induced sepsis. Furthermore, TRPM2-deficient astrocytes (transfected with TRPM2 siRNA) upon LPS stimulation also induced decreased IL-1β, IL-6 and TNF-α level. Our data suggested that decreased production of inflammatory cytokines and apoptosis related proteins with TRPM2 deletion could regulate inflammatory stress and decrease inflammatory injury in hippocampal neurons, and consequently, ameliorate brain disorder.

1. Introduction

Sepsis is one of the most significant challenges presented by bacterium infected patients, surgical patients and trauma victims in intensive care units (ICU) [1,2]. The central nervous system is one of the first organs to be affected by sepsis. Sepsis-associated encephalopathy (SAE) is a transient and reversible brain dysfunction, occurring when the source of sepsis is located outside of the central nervous system. SAE affects approximately a third of septic patients and is a risk factor for long term disability and mortality [3–5]. SAE manifests itself with a range of symptoms ranging from acute impaired attention to confusion, lethargy, delirium and coma [5]. The mechanism underlying SAE involves inflammatory and noninflammatory processes that affect endothelial cells, glial cells and neurons; these processes also disrupt intracellular metabolism and induce a breakdown of the blood-brain barrier [6]. Pathological neuronal loss and increased apoptosis have been reported in various models of sepsis in rodents [7,8], but the mechanism by which the central nervous system dysfunction induced by LPS-induced sepsis has not been defined.

The regulation of calcium (Ca^{2+}) influx across the plasma membrane is crucial for immune responses in the central nervous system. Cytosolic levels of Ca^{2+} control a diverse range of cellular processes,

* Corresponding authors at: Department of Neurology, Zhejiang Key Laboratory for Diagnosis and Treatment of Neonatal Diseases, Children's Hospital, School of Medicine, Zhejiang University, Hangzhou 310052, Zhejiang, China.
E-mail addresses: jiangpeifang@zju.edu.cn (P. Jiang), shuqiang@zju.edu.cn (Q. Shu).

https://doi.org/10.1016/j.intimp.2019.105836
Received 31 May 2019; Received in revised form 1 August 2019; Accepted 17 August 2019
Available online 23 August 2019
1567-5769/

including microglia, astrocyte and oligodendrocyte activation, and the secretion of pro- and anti-inflammatory cytokines [9–11]. Transient receptor potential melastatin 2 (TRPM2, also called TRPC7 or LTRPC2), which is a member of the melastatin subfamily of TRP channels, has been identified as a unique fusion of a Ca^{2+}-permeable nonselective cation channel [12]. It is highly expressed in brain and abundantly in immunocytes including monocytes, neutrophils and macrophages [13,14]. In brain, TRPM2 is indispensable component in the regulation of Ca^{2+} homeostasis significantly impacting the function of astrocyte.

Detailed characterization of TRPM2-genetically deficient mice in different inflammatory models has revealed the involvement of this channel in various aspects of innate immunity. Yamamoto et al. reported that TRPM2 disruption can attenuate macrophage inflammatory protein-2 (CXCL2) expression, neutrophil infiltration and ulceration in the dextran sulfate sodium-induced colitis inflammation model [14]. Di et al. proposed that TRPM2 protects mice through inhibition of the membrane NAPDH-oxidase complex in phagocytic cells in an endotoxin-induced lung inflammation model [15]. In contrast, Knowles et al. proposed that TRPM2 deficient mice are more vulnerable to infection with *Listeria monocytogenes* than wild-type mice [13]. The diversity of these findings suggests that TRPM2 may play distinct roles under different inflammatory situations. It is therefore important to clarify the mechanisms by which TRPM2 activation may exert a pro- or anti-inflammatory function in sepsis-associated encephalopathy (SAE).

TRPM2's sensitivity toward reactive oxygen species (ROS), tumor necrosis factor (TNF)-α, and elevated its intracellular expression suggested that it might be important for inflammatory processes [16,17]. Inflammatory mediators such as IL-1β, IL-6 or TNF-α can induce abnormal neurotransmitter composition of the reticular activating system, impair neuroglia function, and cause neuronal degeneration and necrosis. Thus, we hypothesized that TRPM2 cation channel might be involved in the release of inflammatory mediators and development of neurologic dysfunction during sepsis. However, there have been no reports regarding the effects of TRPM2 cation channel on the cytokines production in astrocytes and brain disorder induced by sepsis.

This study investigated how TRPM2-mediated functions affect neuroethology changes, inflammation mediators release and apoptosis related proteins expressions of LPS infected mouse sepsis model. Our findings reveal that the absence of TRPM2 results in decreased production of inflammation mediators (IL-1β, IL-6, TNF-α) and apoptosis related proteins (BNIP3, AIF and Endo G). The loss of TRPM2 results in decreased hippocampal neurons injury, and consequently, ameliorates brain disorder.

2. Materials and methods

2.1. Animals

Trpm2-knockout (TRPM2-KO) mice were obtained from Department of Synthetic Chemistry and Biological Chemistry, Kyoto University, Japan [18], and they (backcrossed for 12 generations onto the C57BL/6 background) were maintained in our laboratory. The mice used in our study were littermates which were bred from *Trpm2*$^{+/-}$ mice in the Medical Institute Animal Center of Zhejiang University. All experiments were conducted in accordance with the ethical guidelines for animal experiments of Zhejiang University Medical College Ethics Committee. Male mice aged 6–8 weeks and weighing 22-26 g were used in this study. They were group-housed 2–6 mice per cage with free access to food and water and kept at a constant ambient temperature of 24 ± 2 °C under a 12 h light/dark cycle.

2.2. Experimental protocol

The study was designed to include three sets of experiments: 1) assessment of neuroethology, 2) measurements of cytokines, BNIP3, AIF and Endo G in vivo experiment, and 3) studies of TRPM2 transfection in vitro experiment. The in vitro or in vivo experiments were respectively performed 5 times. Sepsis was induced by intraperitoneally (i.p) injection of LPS, as described by Wichterman et al. [19]. Male C57BL/6 WT or *Trpm2*-KO mice were randomly divided into four groups as follows: Group 1, WT-saline group (0.5 mL of saline i.p injected in WT mice, $n = 25$); Group 2, WT-LPS group (LPS [50 mg/kg, Sigma] i.p injected in WT mice, n = 25); Group 3, KO-saline group (0.5 mL of saline i.p injected in *Trpm2*-KO mice, n = 25); Group 4, KO-LPS group (LPS [50 mg/kg, Sigma] i.p injected in *Trpm2*-KO mice, n = 25). In in vivo experiment, we used four groups as follows: the control group (astroglia cell + PBS), TRPM2-siRNA group (astroglia cell + TRPM2-siRNA), LPS group (astroglia cell + PBS + LPS), LPS + TRPM2-siRNA group (astroglia cell + TRPM2-siRNA + LPS).

2.3. Neurologic assessment

Four groups of mice ($n = 10$ per group) were neurologically assessed at 3, 12, 24 and 48 h after LPS injection, as described by Kadoi et al. [20]. The pinna reflex was assessed by lightly touching the auditory meatus of the ear to elicit a head shake (normal, 2 points; weak [loss of reflex for 10 s], 1 point; none [loss of reflex for > 30 s], 0 points). The corneal reflex was evaluated by lightly touching the cornea with a cotton swab to elicit a head shake (normal, 2 points; weak [loss of reflex for 10 s], 1 point; none [loss of reflex for > 30 s], 0 points). The paw or tail flexion reflex was assessed by briefly pinching the hind paw or tail to elicit a withdrawal response (normal, 2 points; weak [loss of reflex for 10 s], 1 point; none [loss of reflex for > 30 s], 0 points). Righting reflex was tested by placing the animal on its back and measuring the time it took to return to a spontaneous upright position (normal, 2 points; weak [loss of reflex for 10 s], 1 point; none [loss of reflex for > 30 s], 0 points). The escape response was assessed by briefly pinching the tail of the animal to elicit locomotive activity away from the noxious stimulus (normal, 2 points; weak [loss of reflex for 10 s], 1 point; none [loss of reflex for > 30 s], 0 points). Maximal obtainable scores were 10 points. The pinna reflex, the corneal reflex, the paw or tail flexion reflex were used to assess simple nonpostural somatomotor function, and the righting reflex, the escape response were to assess complex postural somatomotor function as reported previously. Neurologic assessments were made at the appropriate times by an observer who was blinded to the treatment the mice had received.

2.4. Tissue fixation, histopathological examination and immunofluorescent staining

Four groups of mice ($n = 5$ per group) were i.p injected with chloral hydrate (0.3 ml/100 g) for deep anesthesia and killed at 24 h after treatment with LPS (50 mg/kg) or same volume of saline. Mice were perfused transcardially with 0.9% saline, followed by 10% paraformaldehyde in 0.1 M phosphate-buffered saline (PBS) (pH 7.4). The brains were removed and cut coronally 2–3 mm in front of the ventral optic chiasm and back along the leading edge of the pons. The middle part of brain was immersed in 4% paraformaldehyde and kept at 4 °C in a refrigerator for 24 h. Then, the section was dehydrated in graded ethanol, embedded in paraffin, and coronal serial sections were cut with a slice thickness of 4 μm. Brains were stained with HE to assess for evidence of cyst formation or areas of loss of normal cellular architecture.

For immunofluorescent labeling of glial fibrillary acidic protein (GFAP), markers of glial cells, sections were treated to denaturate DNA (2.4 N HCl for 20 min at 37 °C) and incubated overnight in anti-GFAP (1:1000; Abcam company, UK, Catalog #ab7260) in PBST containing 5% normal goat serum. FITC conjugated secondary antibodies (1:100; Zymed) were added, and the sections were held at 37 °C for 40 min, followed by counterstaining with DAPI for 1 min. Immunofluorescent labeling of TRPM2 (1:1000, Abcam company, UK, Catalog #ab11168) was done as before. Fluorescently labeled sections were imaged by a

Table 1
Sequences of the primers for TNF-α, IL-1β, IL-6 and β-actin.

Gene	Primer	Sequence (5′-3′)
TNF-α	Forward	TACTGAACTTCGGGGTGA
	Reverse	ACTTGGTGGTTTGCTACG
IL-1β	Forward	GGCAGTATCACTCATTGTG
	Reverse	CTCCACTTTGCTCTTGAC
IL-6	Forward	GCCTTCTTGGGACTGATG
	Reverse	AGGTCTGTTGGGAGTGGTA
β-actin	Forward	CTACAATGAGCTGCGTGTG
	Reverse	GCGTGAGGGAGAGCATAG

confocal laserscanning microscope (Zeiss LSM 510 Meta; Carl Zeiss MicroImaging, Inc., Jena, Germany). Images were acquired using Zeiss LSM software.

2.5. Quantitative real-time Polymerase Chain Reaction

Quantitative-PCR amplification was performed in an ABI PRISM 7500 Real-Time PCR System (ABI/PE, Foster City, CA, USA). SYBR Green (TAKARA company, China) was used for the quantitation of PCR reactions. The cDNA was synthesized by MMLV reverse transcriptase (Superscript-Invitrogen, Carlsbad, CA, USA). The sequences of the primers for IL-1β, IL-6 and TNF-α and β-actin (TAKARA company, China) were described in Table 1. β-actin was used as internal control to standardize the amount of cDNA added to the reaction. The real-time PCR was carried out in two steps: (1) initial denaturation at 94 °C for 2 min; (2) 40 cycles at 94 °C for 15 s and 60 °C for 45 s. Reactions without template served as negative controls. The Ct value of the target gene was normalized to the levels of β-actin from the same sample as an internal control. Thus, the ΔCt value was defined as the absolute value of the difference between the Ct value of the target gene and β-actin for each sample. ΔCt = Ct (target gene) - Ct (β-actin). The ΔΔCt was determined by subtracting the mean ΔCt of the control group. We used the $2^{-\Delta\Delta Ct}$ method to calculate target gene changes compared to controls.

2.6. Western blot analysis

Hippocampus tissues corresponding to each group ($n = 5$ per group) were homogenized in RIPA buffer. Samples were centrifuged at 12,000*g* for 5 min at 4 °C. Protein concentration was measured using BCA method. Fifty micrograms protein extracts were resolved on 8–10% SDS polyacrylamide gels and electrotransferred onto polyvinylidene fluoride (PVDF) membranes (Amersham) using a BioRad gel blotting apparatus. Nonspecific binding of antibody was blocked by incubation in 5% milk powder in T-TBS (20 mM Tris-HCl, 150 mM NaCl, 0.1% Tween 20) at room temperature for 2 h. Membranes were incubated overnight at 4 °C with primary antibody (BNIP3 1: 3000, Abcam company, UK, Catalog# 3485-1; AIF 1:1000, Abcam company, UK, Catalog# 3322-1; Endo G 1:2000, Abcam company, UK, Catalog# 2105-1). The next day, the membranes were washed three times in T-TBS (containing 0.1% Tween 20 and TBS buffer) for 10 min each. Membranes were incubated for 2 h with secondary antibody at room temperature and washed three times in T-TBS. To confirm equivalent loading of samples, the same membranes were incubated with β-actin antibody. Peroxidase was visualized by enhanced chemiluminescence (ECL Plus Detection Kit, Beyotime) and exposure to ECL films (Amersham, UK) for appropriate times. The bands of Western blots were quantitated by densitometry and normalized with β-actin using Image Pro Plus software.

2.7. Astrocyte culture and transfection

Culture of primary astrocyte was prepared from the brains of postnatal 1–3 days old C57BL/6 neonatal mice as previously described

Table 2
Neurologic assessment of the four groups of mice (n = 10/group).

	3 h				12 h				24 h				48 h			
	1	2	3	4	1	2	3	4	1	2	3	4	1	2	3	4
Pinna reflex	2 ± 0	1.6 ± 0.2	2 ± 0	1.8 ± 0.1	2 ± 0	0.4 ± 0.2	2 ± 0	0.9 ± 0.2	2 ± 0	1.0 ± 0.1	2 ± 0	1.3 ± 0.2	2 ± 0	1.5 ± 0.2	2 ± 0	1.6 ± 0.2
Corneal reflex	2 ± 0	1.5 ± 0.2	2 ± 0	1.6 ± 0.2	2 ± 0	0.6 ± 0.2	2 ± 0	1.1 ± 0.2	2 ± 0	1.0 ± 0.2	2 ± 0	1.4 ± 0.2	2 ± 0	1.4 ± 0.2	2 ± 0	1.5 ± 0.2
Paw or tail flexion reflex	2 ± 0	1.5 ± 0.2	2 ± 0	1.6 ± 0.2	2 ± 0	0.4 ± 0.2	2 ± 0	0.9 ± 0.2	2 ± 0	1.1 ± 0.1	2 ± 0	1.4 ± 0.2	2 ± 0	1.5 ± 0.2	2 ± 0	1.5 ± 0.2
Righting reflex	2 ± 0	1.5 ± 0.2	2 ± 0	1.6 ± 0.2	2 ± 0	0.3 ± 0.2	2 ± 0	0.7 ± 0.2	2 ± 0	1.2 ± 0.1	2 ± 0	1.5 ± 0.2	2 ± 0	1.6 ± 0.2	2 ± 0	1.6 ± 0.2
Escape response	2 ± 0	1.2 ± 0.1	2 ± 0	1.3 ± 0.2	2 ± 0	0.3 ± 0.2	2 ± 0	0.7 ± 0.2	2 ± 0	1.2 ± 0.1	2 ± 0	1.5 ± 0.2	2 ± 0	1.6 ± 0.2	2 ± 0	1.5 ± 0.2
Total score	10 ± 0	7.1 ± 0.6*	10 ± 0	7.8 ± 0.6*	10 ± 0	2.0 ± 0.6*	10 ± 0	4.3 ± 0.5*▲	10 ± 0	5.5 ± 0.4*	10 ± 0	7.1 ± 0.4*▲	10 ± 0	7.6 ± 0.5*	10 ± 0	7.7 ± 0.4*

1: WT-saline, 2: WT-LPS, 3: KO-saline, 4: KO-LPS.
* $P < 0.05$ vs. WT-saline group.
▲ $P < 0.05$ KO-LPS vs. WT-LPS group.

[21,22]. Briefly, the brains were freed from meninges, and digested enzymatically with 0.25% trypsin (Sigma-Aldrich) and 0.25% DNAse (Roche, Mannheim, Germany). Single cell suspensions obtained were seeded into poly-L-lysine-coated T 75 mm^2 culture flasks in medium consisting of Dulbecco's Modified Eagle's Medium (DMEM) + L-Glutamine + 4.5 g/L D-Glucose (Sigma-Aldrich, St. Louis, MO) supplemented with 10% fetal bovine serum FCS, 50 U/ml penicillin, and 50 µg/ml streptomycin (all Biochrom AG, Berlin, Germany). The cultures were maintained at 37 °C with 5% CO_2 and 95% air. Culture medium was changed every other day. After 10 days, cultures were put on an orbital shaker at 37 °C and 180 rpm for 30 min to remove the microglia. Remaining oligodendrocyte precursor cells were eliminated by shaking at 37 °C and 240 rpm for 6 h in an orbital shaker. Astrocytes were harvested from the culture flasks by mild trypsinization and were replated into 6-well plates at a density of 3×10^5 cells per well. Five days after replating, cultures consisted of at least 95% astrocytes as determined by GFAP (1:1000; Abcam company, UK, Catalog #ab7260) immunofluorescence staining. Astrocytes at approximately 80% confluency were incubated and stimulated with LPS.

Astrocytes (3×10^5 cells/well) were cultured in 6-well plates, and transfected with TRPM2 siRNA (Santa Cruz, America, Catalog #sc-42,674) or empty vector using HiPerFect ®Transfection Reagent (QIAGEN, German) following the manufacturer's instructions. Three candidates of TRPM2 siRNA were initially tested for validation on astrocytes using RT-PCR, and the following sequence was chosen: Sense 5′-[GAUAACAACCUGCGCAUCACCAAUUGG], Antisense 5′-[CCAAUU GGUGAUGCGCAGGUUGUUAUC]. Astrocytes were transfected with TRPM2 siRNA using the gene silencing method as previously described [23].

2.8. MTT assay and cell viability in primary astrocytes

Cell viability was measured by quantitative colorimetric assay with MTT-tetrazolio (MTT), as described previously [24]. Primary astroglia cells (3×10^3 cells/well) were seeded in 96-well plates for 24 h in 5% CO_2 at 37 °C without treatment or treated with Lipopolysaccharide (LPS, Sigma-Aldrich, 10.0 µg/ml). Briefly, after TRPM2 siRNA transfected astroglia cells were incubated for 24 h and 48 h, 50 µl MTT solution (0.5 mg/ml) was added for 4 h incubation respectively. Afterwards, supernatants were removed and cells were solubilized with 150 µl DMSO to detect the intracellular formazan crystals formed in the viable cells. Finally, the absorbance of each well was measured at 550 nm by using an ELISA reader as described by the manufacturer.

2.9. Elisa analysis

Supernatant obtained from in vitro cultures was analyzed for IL-1β (R&D Company, America, Catalog #MLB00C), IL-6 (R&D Company, America, Catalog #M6000B) and TNF-α (R&D Company, America, Catalog #MTA00B) following the guidelines of the manufacturer's protocol.

2.10. Statistical analysis

All data are presented as the means ± SD. To analyze neurologic assessment, IL-1β, IL-6 and TNF-α mRNA expression in astrocytes, the average value of different time point was calculated and evaluated by One-way repeated measures ANOVA. Data from HE, immunofluorescent staining, RT-PCR, Western blot and MTT assay were analyzed using One-way ANOVA followed by the Tukey's Multiple Comparison Test. P value < 0.05 was considered statistically significant.

3. Results

3.1. TRPM2 knockout ameliorates neuroethology in LPS-induced endotoxin sepsis mice

The neurological assessment of the four groups of mice was shown in the Table 2. Neurologic dysfunction appeared approximately 1 h after LPS injection in mouse experimental model. There was significant decrease in the total score of WT-LPS and KO-LPS groups. The pinna reflex, corneal reflex, paw or tail flexion reflex, righting reflex and escape response were all significantly decreased in the WT-LPS and KO-LPS groups compared with WT-saline group at 3, 12, 24 and 48 h after LPS injection (all $^*P < 0.05$). The total score reached the lowest value at 12 h after LPS injection. And the value of total score was notably higher in the KO-LPS group than that in the WT-LPS group at 12 h ($^▲P < 0.05$) and 24 h ($^▲P < 0.05$). In contrast, no significant changes in total score were found in the WT-saline and KO-saline groups (all $P > 0.05$) (Fig. 1).

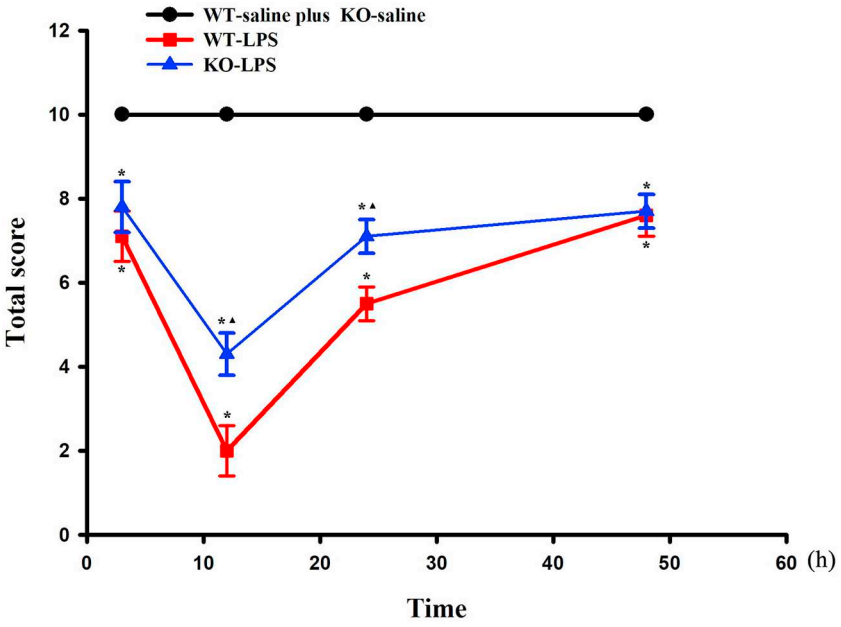

Fig. 1. TRPM2 knockout ameliorates neuroethology in sepsis mice. The total scores are all significantly decreased in the WT-LPS and KO-LPS groups compared with WT-saline group at 3, 12, 24 and 48 h (all $^*P > 0.05$). The total scores of 12 h and 24 h are notably higher in the KO-LPS group than those in the WT-LPS group ($^▲P < 0.05$). In contrast, no significant changes in total score are found in the WT-saline and KO-saline groups (all $^*P > 0.05$).

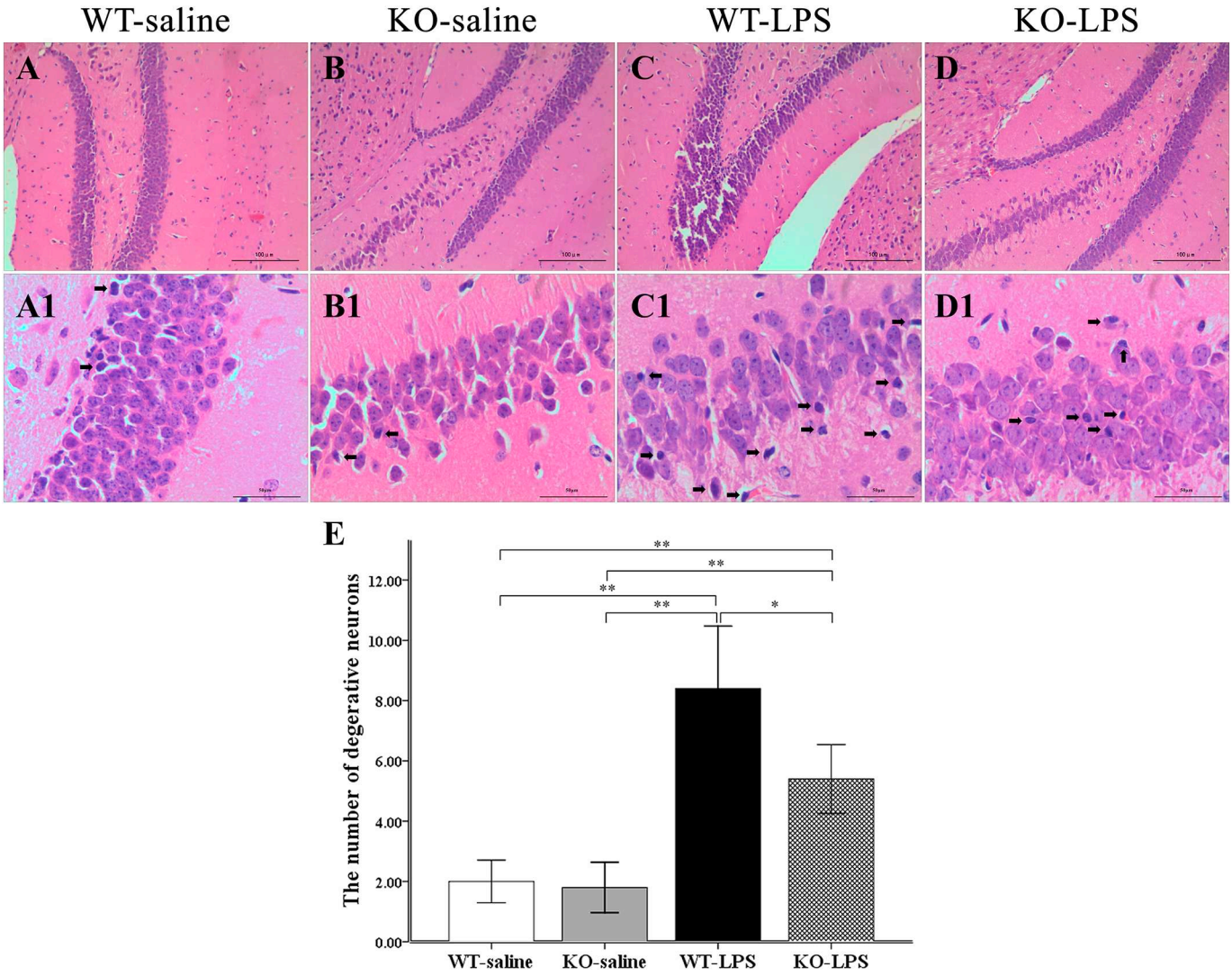

Fig. 2. TRPM2 knockout attenuates pathologic changes in hippocampus. Histological results (10×, 40×) illustrate the pathologic changes in hippocampus. The size and appearance of neurons are normal in the WT-saline (Fig. 1A, A1) and KO-saline (Fig. 1B, B1) groups. Degenerative changes are common in hippocampus of WT-LPS (Fig. 1C, C1) group. Less degenerative changes are found in the KO-LPS (Fig. 1D, D1) group. Quantitative data are expressed as total number of degenerative neurons (Fig. 1E). Scale bars = 100 μm (A-D), 50 μm (A1-D1), Bars represent mean ± SD, *$P < 0.05$, $n = 5$.

3.2. TRPM2 knockout attenuates pathologic changes in hippocampus

Fig. 2 showed the pathologic changes in hippocampus of the four groups of mice. The size and appearance of neurons were normal in the WT-saline (Fig. 2A, A1) and KO-saline (Fig. 2B, B1) groups. Degenerative changes such as pyknotic nuclei of neurons, darker-staining cytoplasm and vacuolization were common in hippocampus of WT-LPS group (Fig. 2C, C1). Less degenerative changes were found in the KO-LPS group (Fig. 2D, D1). The number of degenerative neurons was significantly decreased in KO-LPS group compared to WT-LPS group (WT-saline: 2.00 ± 0.71, KO-saline: 1.80 ± 0.84, WT-LPS: 8.40 ± 2.07, KO-LPS: 5.40 ± 1.14; $F_{(3,16)} = 28.94$, $P < 0.01$) (Fig. 2E).

3.3. TRPM2 knockout reduces GFAP-positive astrocytes in hippocampus

In order to confirm that GFAP reduction by TRPM2 knock-down occurs in mouse brain, we used immunofluorescent staining to examine GFAP expression in hippocampus. Our data showed that TRPM2 knockout mice could show reduction of GFAP-positive astrocytes after LPS administration (WT-LPS: 1204.80 ± 115.90, KO-LPS: 718.00 ± 111.46, $F_{(1,8)} = 45.83$, $P < 0.01$) (Fig. 3).

3.4. TRPM2 knockout decreases IL-1β, IL-6 and TNF-α mRNA expression levels in vivo

One-way ANOVA analysis showed that there was a significant difference of IL-1β mRNA expression in the four groups ($F_{(3,16)} = 9.96$, $P < 0.01$) (Fig. 4A). There was a significant increase of IL-1β mRNA expression in the WT-LPS group among four groups. The IL-1β mRNA expression was significantly decreased in the KO-LPS group compared to the WT-LPS group (WT-saline: 1.00 ± 0.00, WT-LPS: 3.39 ± 1.54, KO-saline: 1.00 ± 0.04, KO-LPS: 1.78 ± 0.41; $F_{(3,16)} = 9.96$, $P < 0.01$) (Fig. 4A). Similar changes were observed in IL-6 mRNA (WT-saline: 1.00 ± 0.00, WT-LPS: 1.49 ± 0.20, KO-saline: 1.00 ± 0.04, KO-LPS: 1.25 ± 0.08; $F_{(3,16)} = 22.67$, $P < 0.01$)

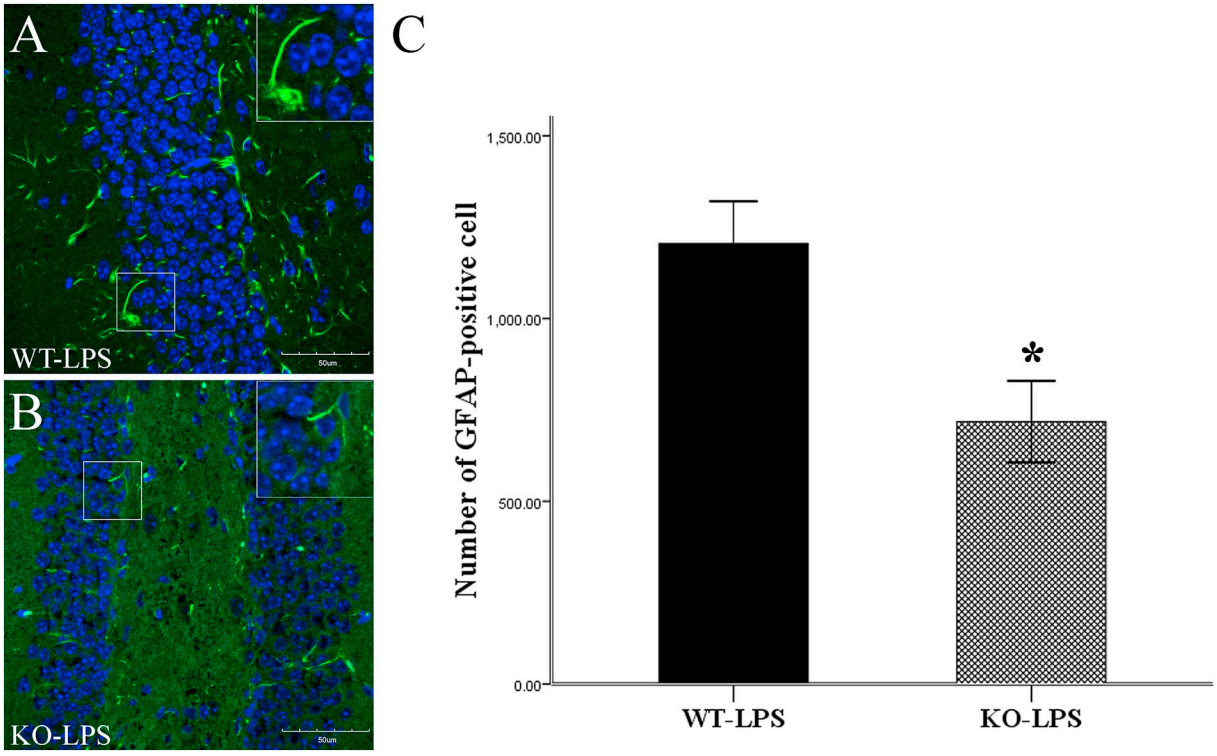

Fig. 3. TRPM2 knockout reduces GFAP-positive astrocytes in hippocampus. Immunofluorescent staining image (40 ×) of GFAP (green) in hippocampus from mice in the (A) WT-LPS, (B) KO-LPS group. Nuclei are counterstained with DAPI (blue). C, Quantitative data are expressed as the total number of GFAP-positive astrocytes. Scale bars = 50 μm, Bars represent mean ± SD. *$P < 0.05$, n = 5. (For interpretation of the references to colour in this figure legend, the reader is referred to the web version of this article.)

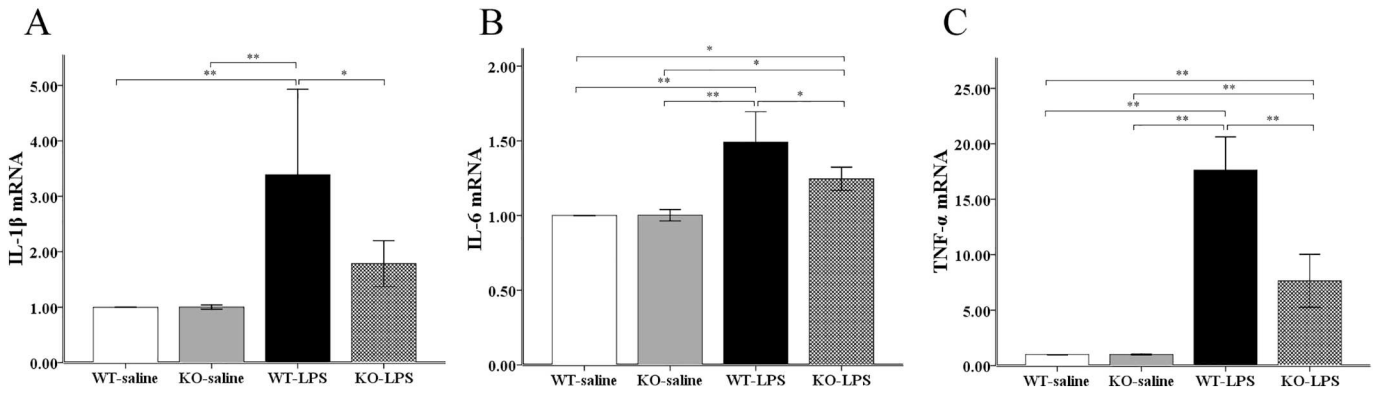

Fig. 4. TRPM2 knockout decreases IL-1β, IL-6 and TNF-α mRNA expression in vivo. The IL-1β (A), IL-6 (B) and TNF-α (C) mRNA expressions are significantly increased in the WT-LPS group. They are significantly decreased in the KO-LPS group compared with the WT-LPS group. Data represents mean ± SD. * $P < 0.05$, n = 5.

(Fig. 4B) and TNF-α mRNA expressions (WT-saline: 1.00 ± 0.00, WT-LPS: 17.63 ± 3.00, KO-saline: 1.00 ± 0.04, KO-LPS: 7.65 ± 2.39; $F_{(3,16)} = 84.06$, $P < 0.01$) (Fig. 4C). The primers of IL-1β, IL-6 and TNF-α were seen in the Table 1.

3.5. TRPM2 knockout decreases BNIP3, AIF and Endo G protein expressions in vivo

To investigate the mechanisms underlying the potential apoptosis in LPS-induced sepsis, we examined the hippocampal expressions of BNIP3, AIF and Endo G protein levels. Western blot analysis showed that there was a significant difference of BNIP3 protein expression in the four groups ($F_{(3,16)} = 176.53$, $P < 0.01$) (Fig. 5A). There was a significant increase of BNIP3 protein expression in the WT-LPS group. The BNIP3 protein expression was significantly decreased in the KO-LPS group compared with the WT-LPS group (WT-saline: 0.88 ± 0.01, KO-saline: 0.82 ± 0.06, WT-LPS: 1.43 ± 0.06, KO-LPS: 0.66 ± 0.07; $F_{(3,16)} = 176.53$, $P < 0.01$) (Fig. 5A). Similar changes were observed

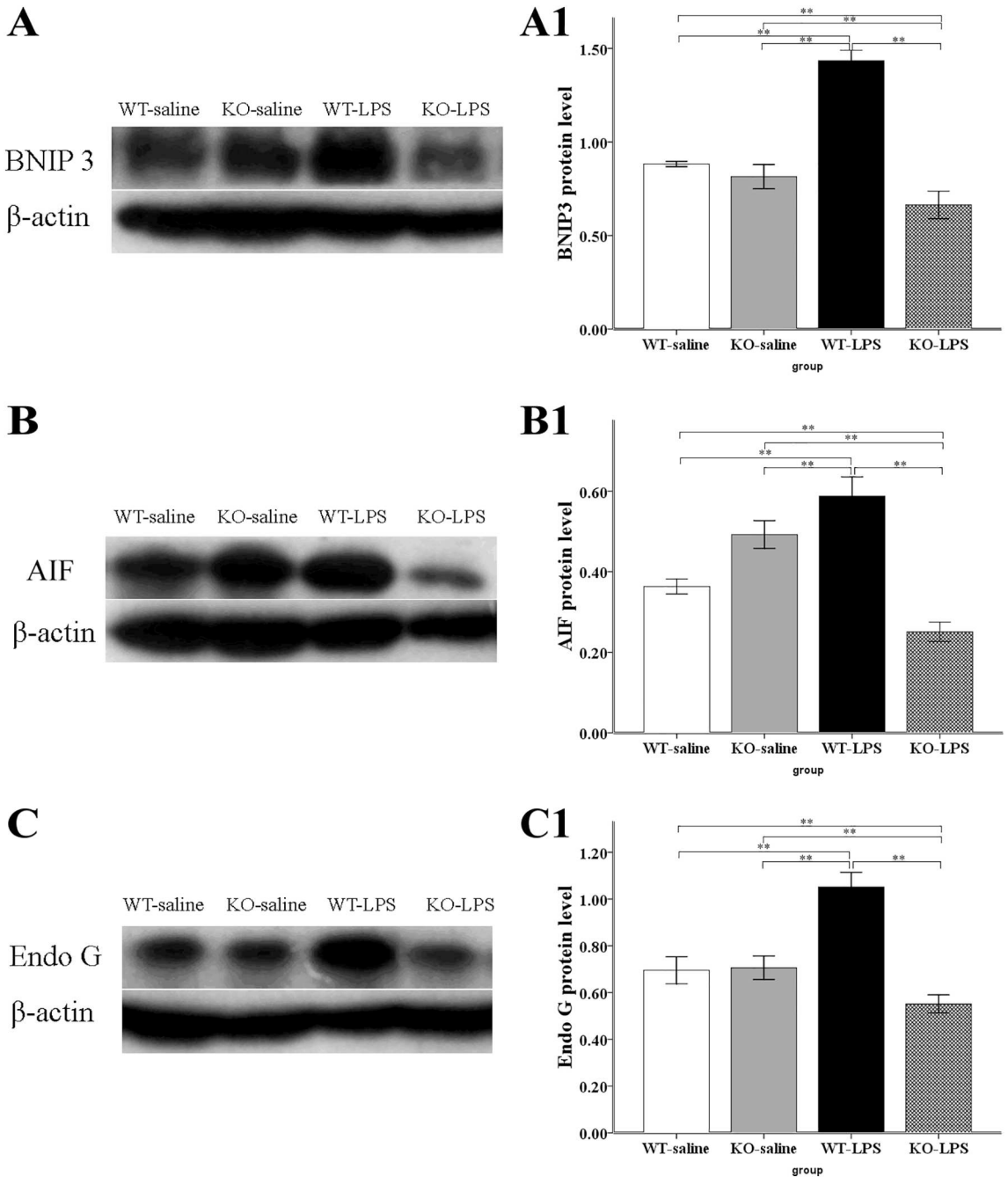

Fig. 5. TRPM2 knockout decreases BNIP3, AIF and Endo G protein expressions in vivo. A representative autoradiograph of BNIP3, AIF and Endo G expression is shown (A-C). Intensities of BNIP3 (A1), AIF (B1) and Endo G (C1) protein bands are quantified by densitometry, respectively. The BNIP3, AIF and Endo G expression are significantly increased in the WT-LPS group. They are significantly decreased in the KO-LPS group compared with the WT-LPS group. Data represents mean ± SD. *$P < 0.05$, n = 5.

in AIF protein (WT-saline: 0.36 ± 0.02, KO-saline: 0.49 ± 0.03, WT-LPS: 0.59 ± 0.05, KO-LPS: 0.25 ± 0.02; $F_{(3,16)} = 98.61$, $P < 0.01$) (Fig. 5B) and Endo G protein expressions (WT-saline: 0.70 ± 0.06, KO-saline: 0.71 ± 0.05, WT-LPS: 1.05 ± 0.06, KO-LPS: 0.55 ± 0.04; $F_{(3,16)} = 80.10$, $P < 0.01$) (Fig. 5C).

3.6. LPS stimulation increases IL-1β, IL-6 and TNF-α levels in astrocyte

We evaluated the effect of LPS on regulation of cytokines production through Elisa analysis. Astrocyte was isolated from WT mice and cultured with or without LPS. After astrocyte culture for 7 days (Fig. 6), we measured IL-1β, IL-6 and TNF-α levels at 2, 6, 12, 24 and 48 h following LPS stimulation. One-way repeated measures ANOVA analysis showed that there was a significant increase of IL-1β level in astrocyte after LPS stimulation. (Fig. 7A). Similar changes were observed in IL-6 (Fig. 7B) and TNF-α level in astrocyte after LPS stimulation (Fig. 7C).

3.7. TRPM2 transfection affects astroglia cell viability, TRPM2 and GFAP expression

We aimed to detect the physiological function of TRPM2 on astroglia cell viability after LPS stimulation. To achieve this goal, we depleted the expression of TRPM2 by its siRNA in astrocyte. Real-time RT-PCR was used to detect the efficacy of TRPM2 siRNA in astroglia cells.

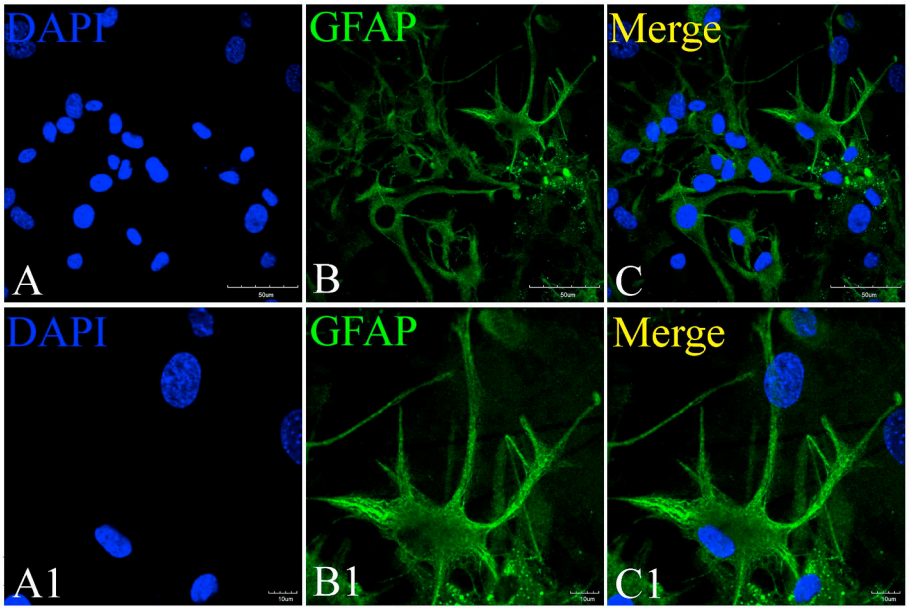

Fig. 6. Identification of primary astroglia cells. Primary astroglia cells are stained with GFAP (green) (B, B1). Nuclei are counterstained with DAPI (blue) (A, A1). Scale bars = 50 μm (63×, A-C); 10 μm (126×, A1-C1). (For interpretation of the references to colour in this figure legend, the reader is referred to the web version of this article.)

The results from our RT-PCR showed that TRPM2 siRNA significantly inhibited the TRPM2 mRNA level in astroglia cells compared to control group. After LPS stimulation, TRPM2 mRNA level in astroglia cells can be significantly increased. However, the increased TRPM2 mRNA level in astroglia cells was remarkably decreased in LPS + TRPM2 siRNA group (Control: 1.00 ± 0.00, TRPM2-siRNA: 0.63 ± 0.09, LPS: 2.80 ± 0.56, LPS + TRPM2-siRNA: 1.44 ± 0.41; $F_{(3,16)} = 36.32$, $P < 0.01$) (Fig. 8). In line with this, our Western blot results identified that TRPM2 siRNA remarkably suppressed the expression of GFAP in astroglia cells (Fig. 9A). The GFAP protein expression was less in the LPS + TRPM2-siRNA group than that in the LPS group. (Control: 0.88 ± 0.12, TRPM2-siRNA: 0.94 ± 0.07, LPS: 1.73 ± 0.20, LPS + TRPM2-siRNA: 1.06 ± 0.14; $F_{(3,16)} = 41.57$, $P < 0.01$) (Fig. 9B).

To explore whether downregulation of TRPM2 affect astroglia cell viability, we performed cell viability assay by MTT in astrocytes transfected with TRPM2 siRNA. The results from MTT showed that there was no significant difference in astroglia cell viability between control and TRPM2 siRNA group. After LPS stimulation for 24 h, astroglia cell viability of the LPS group was higher than the Control group. Downregulation of TRPM2 could inhibit astroglia cell viability in the LPS + TRPM2-siRNA group and showed no significant difference with Control group (Control: 100.24 ± 4.54, TRPM2-siRNA: 91.06 ± 5.28, LPS: 121.10 ± 9.32, LPS + TRPM2-siRNA: 103.80 ± 5.64; $F_{(3,16)} = 18.89$, $P < 0.01$) (Fig. 10A). After LPS stimulation for 48 h, astroglia cell viability was significantly decreased in the LPS group. However, downregulation of TRPM2 could ameliorate astroglia cell viability (Control: 100.20 ± 6.94, TRPM2-siRNA: 97.95 ± 4.21, LPS: 78.82 ± 7.27, LPS + TRPM2-siRNA: 93.58 ± 9.49; $F_{(3,16)} = 8.85$, $P < 0.01$) (Fig. 10B).

3.8. TRPM2 transfection deceases IL-1β, IL-6 and TNF-α level in astrocyte after LPS stimulation

We examined the effect of TRPM2 transfection on IL-1β level in astrocyte after LPS stimulation. One-way ANOVA analysis showed that there was no significant change of IL-1β level in the control group and TRPM2-siRNA group. A significant increase of IL-1β appeared in the LPS group compared to Control and TRPM2-siRNA groups. After TRPM2 transfection, there was a notable decrease of IL-1β in the LPS + TRPM2-siRNA group (Control: 84.90 ± 10.95, TRPM2-siRNA: 48.10 ± 17.43, LPS: 832.20 ± 176.75, LPS + TRPM2-siRNA: 534.80 ± 171.25; $F_{(3,36)} = 93.04$, $P < 0.01$) (Fig. 11A). Similar results were found in IL-6 level (Control: 59.80 ± 13.46, TRPM2-siRNA: 26.70 ± 2.50, LPS: 1604.00 ± 183.77, LPS + TRPM2-siRNA: 1230.40 ± 208.48; $F_{(3,36)} = 337.22$, $P < 0.01$) (Fig. 11B) and TNF-α level (Control: 79.20 ± 11.32, TRPM2-siRNA: 45.20 ± 8.72, LPS: 191.70 ± 10.07, LPS + TRPM2-siRNA: 145.70 ± 20.68; $F_{(3,36)} = 235.99$, $P < 0.01$) (Fig. 11C) in astrocyte after TRPM2 transfection.

4. Discussion

Sepsis associated encephalopathy (SAE) is a diffuse cerebral dysfunction resulted by systemic inflammatory response. Although the mechanism of the cerebral dysfunction is unclear, the central nervous system was proved to be one of the first organs to be affected by sepsis. The primary clinical feature of SAE is a change in mental status. Mildly encephalopathy patients demonstrate an acute fluctuating confusional state and inappropriate behavior. However, more severe patients show delirium, agitation or coma. The SAE can be classified as early-onset septic encephalopathy that presents before multiple organ failure (MOF) occurs and lately-onset encephalopathy that is accompanied by MOF such as hypotension, respiratory failure and other systemic phenomena [25]. The clinical cardinal feature of SAE is a diffuse disturbance in cerebral function without clinical or laboratory evidence of direct brain infection. In spite of the high mortality rate associated with this condition, there is no prophylactic or targeted therapy to reduce or minimize brain damage in septic patients and clinical management is limited to the treatment of the underlying infection [3].

LPS is widely accepted as a model of endotoxin-mediated inflammation, which can mimic the natural response to an infection.

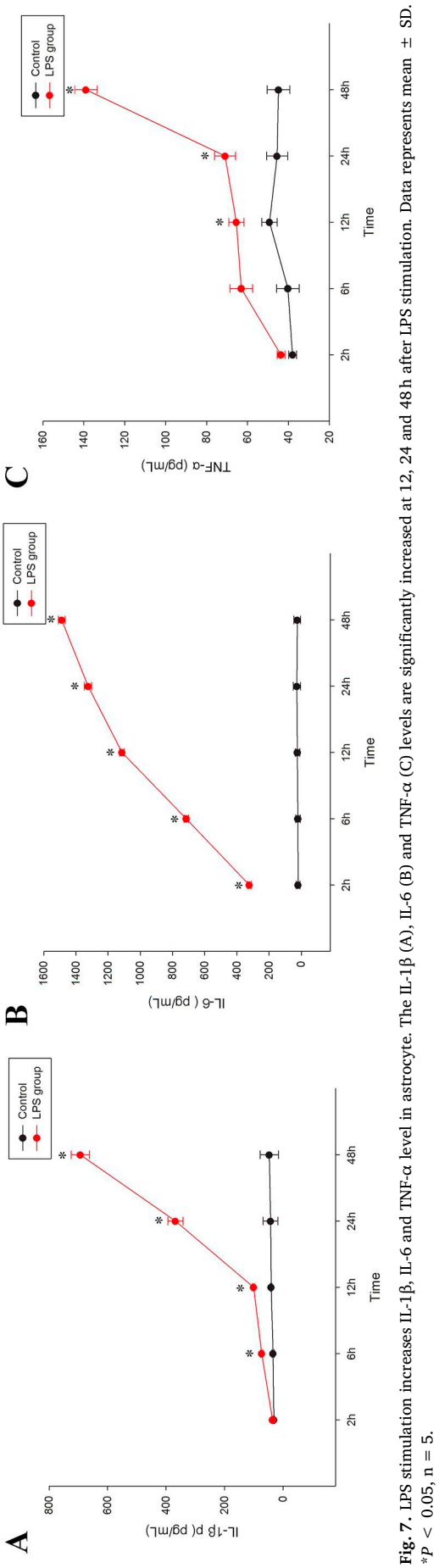

Fig. 7. LPS stimulation increases IL-1β, IL-6 and TNF-α level in astrocyte. The IL-1β (A), IL-6 (B) and TNF-α (C) levels are significantly increased at 12, 24 and 48 h after LPS stimulation. Data represents mean ± SD. *$P < 0.05$, n = 5.

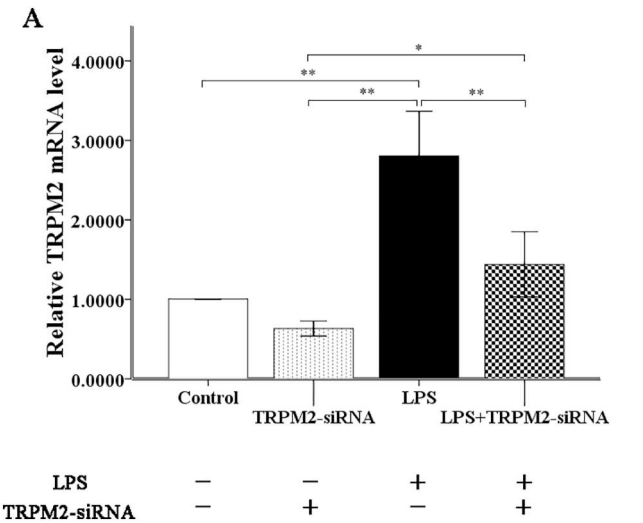

Fig. 8. TRPM2 transfection affects TRPM2 expression in astrocyte. TRPM2 mRNA is significantly increased after LPS stimulation. The TRPM2 mRNA level in LPS + TRPM2 siRNA group is less than that in the LPS group (A). Data represents mean ± SD. *$P < 0.05$, n = 5.

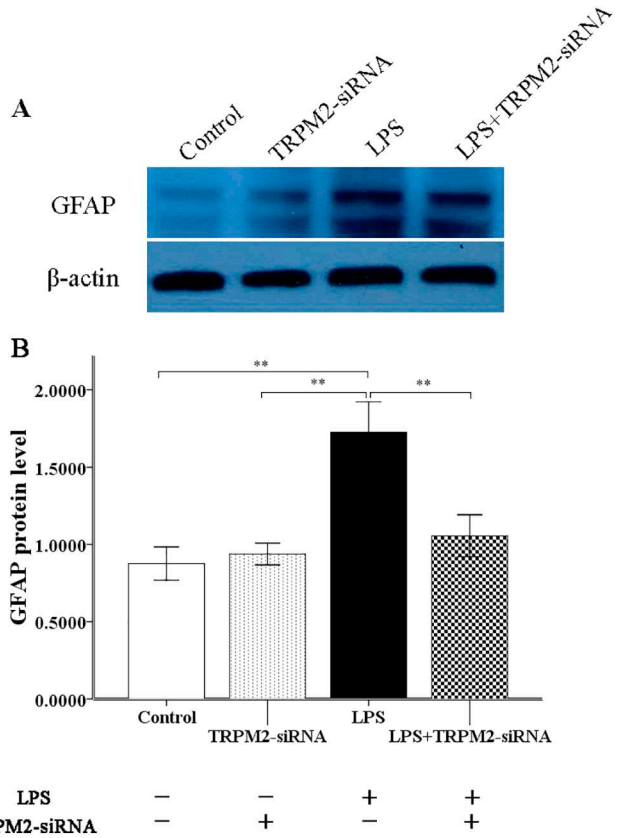

Fig. 9. TRPM2 transfection affects GFAP expression in astrocyte. A representative autoradiograph of GFAP expression is shown (A). Intensities of GFAP protein band were quantified by densitometry (B). GFAP expression is significantly increased after LPS stimulation. The GFAP expression in LPS + TRPM2 siRNA group is less than that in the LPS group (B). Data represents mean ± SD. *$P < 0.05$, n = 5.

Furthermore, TRPM2 channel has been found to be implicated in neuronal damage induced by oxidative stress and traumatic brain injury processes such as inflammation and neuronal death [26–28]. In this study, we used LPS (50 mg/kg, i.p. injection) induced endotoxin sepsis

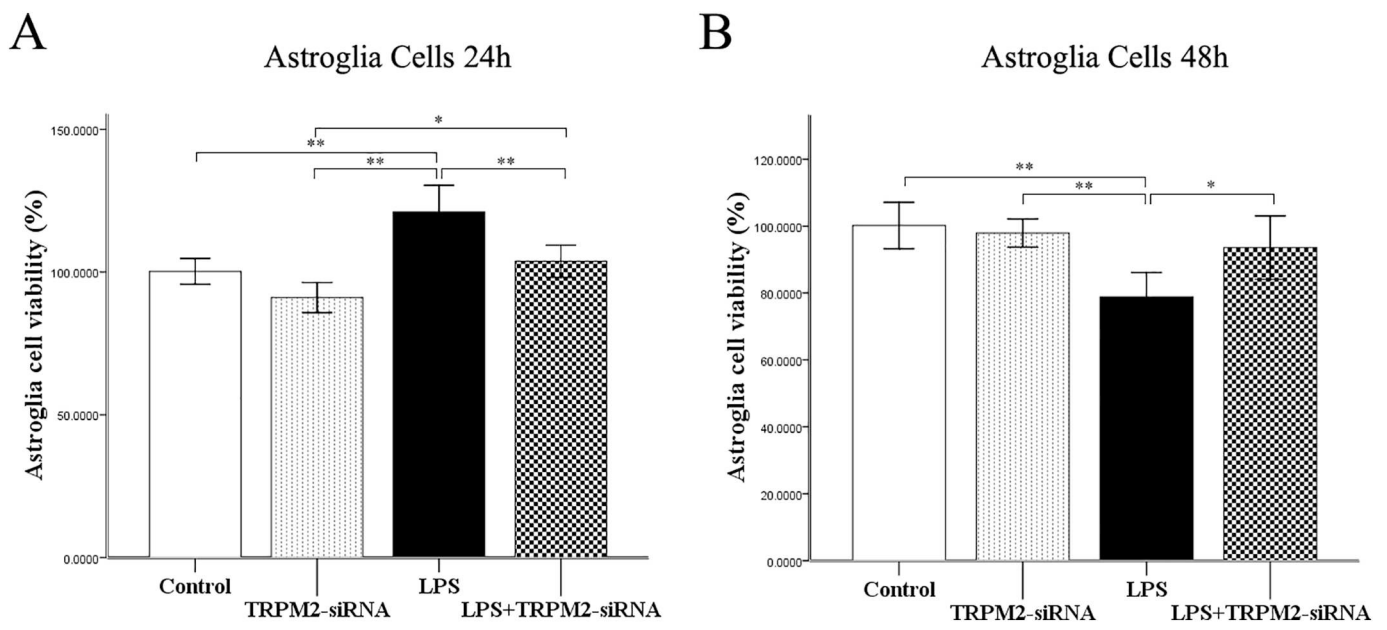

Fig. 10. TRPM2 transfection affects astroglia cell viability. A. MTT assay is conducted to measure cell growth in astroglia cells transfected with TRPM2 siRNA after LPS stimulation for 24 h. B. MTT assay is conducted to measure cell growth in astroglia cells transfected with TRPM2 siRNA after LPS stimulation for 48 h. Data represents mean ± SD. *$P < 0.05$, n = 5.

model to investigate how TRPM2 affects inflammation and oxidative stress responses. Neurologic dysfunction was observed approximately 1 h in mouse experimental model. And the degree of neurologic impairment achieved to the most serious level at 12 h after i.p. injection of LPS. Our data demonstrate that TRPM2 KO mice exhibit higher scores in the pinna reflex, corneal reflex, paw or tail flexion reflex, righting reflex and escape response as compared to WT mice after LPS injection. The neurologic dysfunction was significantly attenuated by genetic disruption of TRPM2. Therefore, we suggest that TRPM2 may play a crucial role in aggravating sepsis-induced neuro-behavioral changes.

Development of SAE probably involves a number of mechanisms, including reduced cerebral blood flow and oxygen extraction, altered blood-brain barrier and cerebral neurotransmission composition, cerebral edema, cerebral inflammation with leukocyte infiltration, neuronal degeneration and activation of glial cell [29–32]. Although the pathophysiology of sepsis and SAE remains unclear and various mechanisms have been proposed, it is well established that apoptosis is an important mechanism during the immunopathogenesis of sepsis [33–35]. Indeed, increased apoptotic death of neurons has been shown in various brain regions in response to sepsis [36,37]. In this study, we found obvious inflammation-mediated hippocampal neurological damage, pyknotic nuclei of neurons, darker-staining cytoplasm and vacuolization in the sepsis model. Furthermore, we found that knockout of TRPM2 could robustly ameliorate LPS-induced hippocampal neuronal pathologic changes. Therefore, we suggest that TRPM2 may play a crucial role in aggravating sepsis-induced hippocampal neuronal injury which is closely associated with neurologic dysfunction.

During evolutionary process of sepsis, neutrophils engulf and kill pathogens primarily through the generation of reactive oxygen species (ROS) [38]. TRPM2 is an intracellular ROS sensor that transduces information to activate Ca^{2+} influx and regulate the membrane potential [12,39]. TRPM2 plays a role in regulating several key functions of inflammation, including specific aspects of the innate immune response and apoptosis [13,14,18,40]. Binding of the second messengers ADP ribose (ADPR), nicotinamide adenine dinucleotide (NAD), and H_2O_2 to TRPM2 activates gating through the TRPM2 channel [41–44]. Many research groups had previously attempted to elucidate the effects of TRPM2 in distinct models of inflammation or infection. Kaneko et al. reported that TRPM2 expressed in rat cortical neurons is critically involved in H_2O_2-induced Ca^{2+} influx that causes neuronal cell death, it is then possible that Ca^{2+} overload may participate in the development of Alzheimer's disease [45]. Cook et al. reported increases in TRPM2 mRNA and protein expression in cortical and hippocampal neurons of experimental traumatic brain injury [46]. Wehrhahn et al. reported that the exposure to LPS led to increased TRPM2 expression in monocytes and TRPM2-mediated Ca^{2+} influx induced the production of pro-inflammatory cytokines such as IL-6, IL-8 and TNF-α, which might contribute to the exacerbation of inflammation [47]. Because TRPM2 has been extensively proposed as an oxidative stress sensor and LPS infection can causes oxidative stress in the brain, we addressed the function of TRPM2 using 50 mg/kg LPS i.p. injection as our endotoxin sepsis model. Inflammatory cytokines such as TNF-α and IL-1β, IL-6, and complement system are the final common pathway in the pathophysiology of brain dysfunction in SAE. TNF-α induces neutrophil infiltration of the brain tissue, alteration in blood-brain barrier, neuronal cell apoptosis, and brain edema. IL-1 and IL-6 stimulates the production of prostaglandin E-2 by brain endothelial cells, which is responsible for the activation of hypothalamus pituitary adrenal axis, thereby causing fever and behavioral alterations [48]. Our findings show that the loss of TRPM2 results decreased IL-1β, IL-6 and TNF-α mRNA expression in hippocampus, indicating TRPM2 has a regulatory, pro-inflammatory function.

Bcl-2/E1B-19 K-interacting protein 3 (BNIP-3) is a BH3-only pro-apoptotic member of the Bcl-2 family: it mediates cell death via different pathways, including the mitochondrial pathway [49,50]. Apoptosis-inducing factor (AIF) is a mitochondrial protein that translocates to the cytosol and the nucleus, mediating caspase-independent apoptosis in a number of model systems [51–55]. Mitochondrial endonuclease G (Endo G) participates in mitochondrial DNA copying, recombination, and repair [56,57], induced by oxidative stress, it

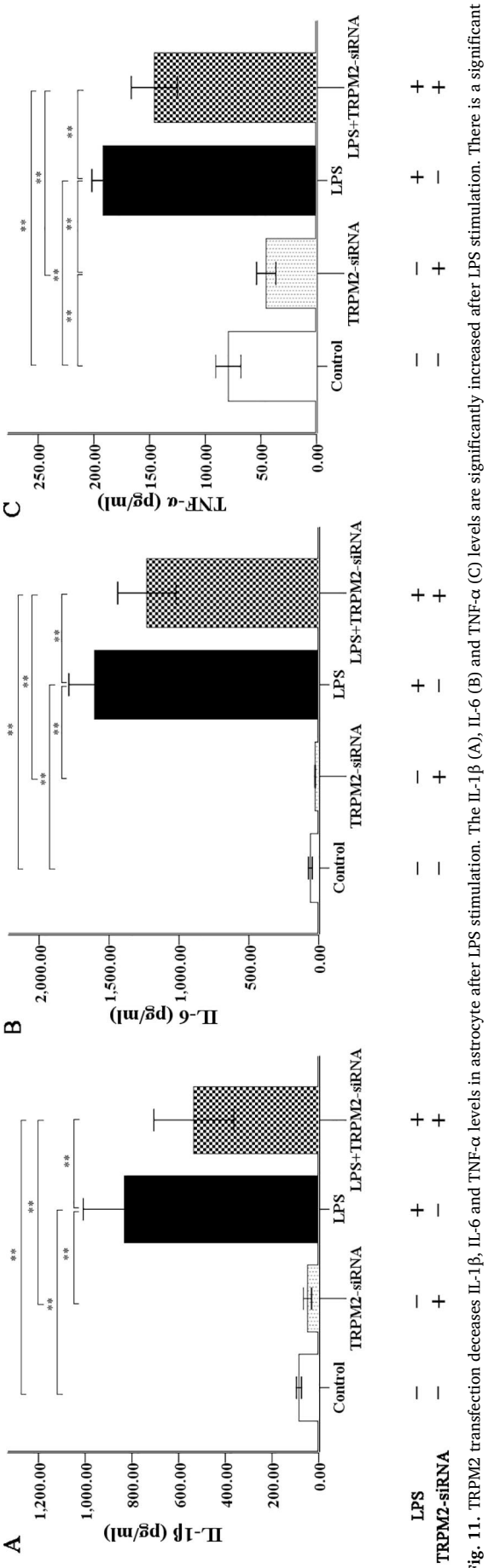

Fig. 11. TRPM2 transfection deceases IL-1β, IL-6 and TNF-α levels in astrocyte after LPS stimulation. The IL-1β (A), IL-6 (B) and TNF-α (C) levels are significantly increased after LPS stimulation. There is a significant decrease of IL-1β, IL-6 and TNF-α levels in LPS + TRPM2 siRNA group compared with those in the LPS group. Data represents mean ± SD. $^{*}P < 0.05$, n = 5.

translocates from the mitochondria to the nucleus [58]. Many research groups had previously attempted to elucidate the role of BNIP-3, AIF and Endo G in caspase-independent pathways. Parrish et al. reported that cps-6 encodes a homologue of Endo G, which is the first mitochondrial protein identified to be involved in programmed cell death in *C. elegans*, underscoring the conserved and important role of mitochondria in the execution of apoptosis [59]. Wang et al. proposed that Endo G released from the mitochondria interacts with AIF in the nucleus and is involved in caspase-independent apoptosis in *Caenorhabditis elegans* [60]. Liu et al. reported that BNIP-3 silencing significantly prevented AIF and Endo G translocation and decreased the apoptosis rate, cytochrome *c* release, and caspase-9 and caspase-3 activation [61]. In our study, data also support the finding that TRPM2 KO mice demonstrated decreased levels of apoptosis related proteins (BNIP3, AIF and Endo G) compared to WT mice, indicating TRPM2 has a regulatory, pro-apoptotic function. TRPM2 may be involved in the caspase-independent apoptotic pathway and it is located upstream of BNIP-3/AIF/Endo G.

TRPM2, a nonselective Ca^{2+}-permeable channel is abundantly expressed in the brain, both in microglia, astroglia and neuronal cells. Bond et al. reported that TRPM2 calcium channel expression in astroglia cells could be up-regulated in response to oxidative stress [62]. Astrocytes which form perivascular endfeet at the blood-brain barrier (BBB) have a particular role in ionic, neurotransmitter and water homeostasis of the brain [63]. Bowman et al. found that the level of expression of messenger RNA for Toll-like receptors 4 (TLR4) on primary murine astrocytes is markedly elevated while exposed to LPS, which suggested that TLRs can directly recognize highly conserved bacterial components in astrocytes endfeet and attribute to the action of cytokines and other acute phase reactants [64]. Because TRPM2 does correlate closely with astroglia cells activation in inflammation, we addressed TRPM2 and GFAP expression in astrocytes after TRPM2 transfection. Our findings show that TRPM2 transfection decreases TRPM2 mRNA and GFAP protein expressions in astrocyte after LPS stimulation. Data also support the finding that TRPM2 transfection astrocytes demonstrated decreased IL-1β, IL-6 and TNF-α level after LPS stimulation, indicating TRPM2 has pro-inflammatory function in astrocytes.

In summary, it is clear that regulation of inflammation response by TRPM2 channel is vital for controlling brain disorder in sepsis-associated encephalopathy. Here using LPS-induced endotoxin sepsis model, we provide novel insight into immune regulation by astrocytes via the nonselective cation channel TRPM2. The absence of TRPM2 results in improved neuroethology, and remissive pathologic changes in hippocampus and decreased inflammatory cytokines (IL-1β, IL-6 and TNF-α) and apoptosis related proteins (BNIP3, AIF and Endo G) in TRPM2 KO mice. The transfection of TRPM2 in astrocytes decreased production of IL-1β, IL-6 and TNF-α in response to LPS stimulation. Our data suggest that inhibition of TRPM2 function may provide a therapeutic strategy to control excessive inflammation activity and reduce brain damage. Alternatively, inhibition of TRPM2 could decrease inflammation mediated astrocytes activation and pro-inflammatory secretion during infection. The mechanisms of astrocyte in infection-mediated brain damage has the potential to open doors to identifying many molecules that might serve as novel therapeutic targets for a wide range of neurological disorders. Further studies are required to understand the mechanisms of TRPM2 calcium channel functional expression in astroglia cells in response to LPS.

In this study, we use a total KO mouse and there are some limitations of our data. Constitutive KO of TRMP2 lacks temporal and spatial resolution. Constitutive KO of TRMP2 affects neuron development showing impaired neuron plasticity and increased neurite outgrowth, which may result in a distinguished baseline before inducing the LPS-induced endotoxin sepsis model [65]. To avoid such potential dilemma, conditional KO TRMP2 right before the induction of the model or when the mice reach adulthood would be ideal. In future studies, conditional

KO TRMP2 in different cell types (e.g., neuron, astrocytes, microglia) are also needed to dissect and confirm the source of various cytokines in vivo.

Acknowledgments

The work of the authors is supported by Grants from National Natural Science Foundation of China (81201511, 81372116, 81671287), Zhejiang Provincial Natural Science Foundation of China (LY15H090006, LY17H040001), Zhejiang Basic Public Welfare Research Project (2019ZD032). The TRPM2 KO mice were kindly provided by Pr. Fang Xiangming from Department of Synthetic Chemistry and Biological Chemistry, Kyoto University, Japan. We are grateful to Pr. Fang Xiangming who helped us to successfully complete this research work.

Declaration of competing interest

The authors declare that no conflict of interest exists.

References

[1] J.P. Donnelly, M.M. Safford, N.I. Shapiro, J.W. Baddley, H.E. Wang, Application of the third international consensus definitions for sepsis (Sepsis-3) classification: a retrospective population-based cohort study, Lancet Infect. Dis. 17 (6) (2017) 661–670.
[2] M. Singer, C.S. Deutschman, C.W. Seymour, M. Shankar-Hari, D. Annane, M. Bauer, R. Bellomo, G.R. Bernard, J.D. Chiche, C.M. Coopersmith, R.S. Hotchkiss, M.M. Levy, J.C. Marshall, G.S. Martin, S.M. Opal, G.D. Rubenfeld, T. van der Poll, J.L. Vincent, D.C. Angus, The third international consensus definitions for sepsis and septic shock (Sepsis-3), JAMA 315 (8) (2016) 801–810.
[3] C. Robba, I.A. Crippa, F.S. Taccone, Septic encephalopathy, Curr Neurol Neurosci Rep 18 (12) (2018) 82.
[4] N. Heming, A. Mazeraud, F. Verdonk, F.A. Bozza, F. Chretien, T. Sharshar, Neuroanatomy of sepsis-associated encephalopathy, Crit. Care 21 (1) (2017) 65.
[5] P.P. Pandharipande, T.D. Girard, J.C. Jackson, A. Morandi, J.L. Thompson, B.T. Pun, N.E. Brummel, C.G. Hughes, E.E. Vasilevskis, A.K. Shintani, K.G. Moons, S.K. Geevarghese, A. Canonico, R.O. Hopkins, G.R. Bernard, R.S. Dittus, E.W. Ely, B.-I.S. Investigators, Long-term cognitive impairment after critical illness, N. Engl. J. Med. 369 (14) (2013) 1306–1316.
[6] R.S. Hotchkiss, L.L. Moldawer, S.M. Opal, K. Reinhart, I.R. Turnbull, J.L. Vincent, Sepsis and septic shock, Nat Rev Dis Primers 2 (2016) 16045.
[7] G.B. Young, Programmed neuronal death in sepsis: caught in a crossfire or a planned sacrifice? Crit. Care Med. 32 (8) (2004) 1804–1805.
[8] E. Messaris, N. Memos, E. Chatzigianni, M.M. Konstadoulakis, E. Menenakos, S. Katsaragakis, C. Voumvourakis, G. Androulakis, Time-dependent mitochondrial-mediated programmed neuronal cell death prolongs survival in sepsis, Crit. Care Med. 32 (8) (2004) 1764–1770.
[9] G.E. Stutzmann, I. Smith, A. Caccamo, S. Oddo, F.M. Laferla, I. Parker, Enhanced ryanodine receptor recruitment contributes to Ca2+ disruptions in young, adult, and aged Alzheimer's disease mice, J. Neurosci. 26 (19) (2006) 5180–5189.
[10] T.C. Foster, Calcium homeostasis and modulation of synaptic plasticity in the aged brain, Aging Cell 6 (3) (2007) 319–325.
[11] J. Miyanohara, M. Kakae, K. Nagayasu, T. Nakagawa, Y. Mori, K. Arai, H. Shirakawa, S. Kaneko, TRPM2 channel aggravates CNS inflammation and cognitive impairment via activation of microglia in chronic cerebral hypoperfusion, J. Neurosci. 38 (14) (2018) 3520–3533.
[12] D.E. Clapham, TRP channels as cellular sensors, Nature 426 (6966) (2003) 517–524.
[13] H. Knowles, J.W. Heizer, Y. Li, K. Chapman, C.A. Ogden, K. Andreasen, E. Shapland, G. Kucera, J. Mogan, J. Humann, L.L. Lenz, A.D. Morrison, A.L. Perraud, Transient Receptor Potential Melastatin 2 (TRPM2) ion channel is required for innate immunity against listeria monocytogenes, Proc. Natl. Acad. Sci. U. S. A. 108 (28) (2011) 11578–11583.
[14] S. Yamamoto, S. Shimizu, S. Kiyonaka, N. Takahashi, T. Wajima, Y. Hara, T. Negoro, T. Hiroi, Y. Kiuchi, T. Okada, S. Kaneko, I. Lange, A. Fleig, R. Penner, M. Nishi, H. Takeshima, Y. Mori, TRPM2-mediated Ca2+influx induces chemokine production in monocytes that aggravates inflammatory neutrophil infiltration, Nat. Med. 14 (7) (2008) 738–747.
[15] A. Di, X.P. Gao, F. Qian, T. Kawamura, J. Han, C. Hecquet, R.D. Ye, S.M. Vogel, A.B. Malik, The redox-sensitive cation channel TRPM2 modulates phagocyte ROS production and inflammation, Nat. Immunol. 13 (1) (2011) 29–34.
[16] S. Roberge, J. Roussel, D.C. Andersson, A.C. Meli, B. Vidal, F. Blandel, J.T. Lanner, J.Y. Le Guennec, A. Katz, H. Westerblad, A. Lacampagne, J. Fauconnier, TNF-alpha-mediated caspase-8 activation induces ROS production and TRPM2 activation in adult ventricular myocytes, Cardiovasc. Res. 103 (1) (2014) 90–99.
[17] B.A. Miller, J.Y. Cheung, TRPM2 protects against tissue damage following oxidative stress and ischaemia-reperfusion, J. Physiol. 594 (15) (2016) 4181–4191.
[18] M. Tsutsui, R. Hirase, S. Miyamura, K. Nagayasu, T. Nakagawa, Y. Mori, H. Shirakawa, S. Kaneko, TRPM2 exacerbates central nervous system inflammation in experimental autoimmune encephalomyelitis by increasing production of CXCL2 chemokines, J. Neurosci. 38 (39) (2018) 8484–8495.
[19] K.A. Wichterman, A.E. Baue, I.H. Chaudry, Sepsis and septic shock–a review of laboratory models and a proposal, J. Surg. Res. 29 (2) (1980) 189–201.
[20] Y. Kadoi, H. Hinohara, F. Kunimoto, S. Saito, F. Goto, Cannabinoid antagonist AM 281 reduces mortality rate and neurologic dysfunction after cecal ligation and puncture in rats, Crit. Care Med. 33 (11) (2005) 2629–2636.
[21] H. Ikeshima-Kataoka, Y. Matsui, T. Uede, Osteopontin is indispensable for activation of astrocytes in injured mouse brain and primary culture, Neurol. Res. 40 (12) (2018) 1071–1079.
[22] Y. Zhao, C. Luo, J. Chen, Y. Sun, D. Pu, A. Lv, S. Zhu, J. Wu, M. Wang, J. Zhou, Z. Liao, K. Zhao, Q. Xiao, High glucose-induced complement component 3 up-regulation via RAGE-p38MAPK-NF-kappaB signalling in astrocytes: in vivo and in vitro studies, J. Cell. Mol. Med. 22 (12) (2018) 6087–6098.
[23] K.H. Ki, D.Y. Park, S.H. Lee, N.Y. Kim, B.M. Choi, G.J. Noh, The optimal concentration of siRNA for gene silencing in primary cultured astrocytes and microglial cells of rats, Korean J Anesthesiol 59 (6) (2010) 403–410.
[24] B. Gargouri, N.M. Yousif, M. Bouchard, H. Fetoui, B.L. Fiebich, Inflammatory and cytotoxic effects of bifenthrin in primary microglia and organotypic hippocampal slice cultures, J. Neuroinflammation 15 (1) (2018) 159.
[25] S. Cotena, O. Piazza, Sepsis-associated encephalopathy, Transl Med UniSa 2 (2012) 20–27.
[26] Z. Huang, C. Cheng, L. Jiang, Z. Yu, F. Cao, J. Zhong, Z. Guo, X. Sun, Intraventricular apolipoprotein ApoJ infusion acts protectively in traumatic brain injury, J. Neurochem. 136 (5) (2016) 1017–1025.
[27] V. Yuruker, M. Naziroglu, N. Senol, Reduction in traumatic brain injury-induced oxidative stress, apoptosis, and calcium entry in rat hippocampus by melatonin: possible involvement of TRPM2 channels, Metab. Brain Dis. 30 (1) (2015) 223–231.
[28] M. Naziroglu, TRPM2 cation channels, oxidative stress and neurological diseases: where are we now? Neurochem. Res. 36 (3) (2011) 355–366.
[29] F.S. Taccone, S. Scolletta, F. Franchi, K. Donadello, M. Oddo, Brain perfusion in sepsis, Curr. Vasc. Pharmacol. 11 (2) (2013) 170–186.
[30] S.J. Kuperberg, R. Wadgaonkar, Sepsis-associated encephalopathy: the blood-brain barrier and the sphingolipid rheostat, Front. Immunol. 8 (2017) 597.
[31] M.S. Hernandes, J.C. D'Avila, S.C. Trevelin, P.A. Reis, E.R. Kinjo, L.R. Lopes, H.C. Castro-Faria-Neto, F.Q. Cunha, L.R. Britto, F.A. Bozza, The role of Nox2-derived ROS in the development of cognitive impairment after sepsis, J. Neuroinflammation 11 (2014) 36.
[32] M. Michels, L.G. Danieslki, A. Vieira, D. Florentino, D. Dall'Igna, L. Galant, B. Sonai, F. Vuolo, F. Mina, B. Pescador, D. Dominguini, T. Barichello, J. Quevedo, F. Dal-Pizzol, F. Petronilho, CD40-CD40 ligand pathway is a major component of acute neuroinflammation and contributes to long-term cognitive dysfunction after sepsis, Mol. Med. 21 (2015) 219–226.
[33] Y. Yao, H. Deng, P. Li, J. Zhang, J. Zhang, D. Wang, S. Li, Y. Luo, Z. Wei, G. Bi, X.P. Yang, Z.H. Tang, Alpha-lactose improves the survival of septic mice by blockade of TIM-3 signaling to prevent NKT cell apoptosis and attenuate cytokine storm, Shock 47 (3) (2017) 337–345.
[34] C. Cheyuo, A. Jacob, R. Wu, M. Zhou, L. Qi, W. Dong, Y. Ji, W.W. Chaung, H. Wang, J. Nicastro, G.F. Coppa, P. Wang, Recombinant human MFG-E8 attenuates cerebral ischemic injury: its role in anti-inflammation and anti-apoptosis, Neuropharmacology 62 (2) (2012) 890–900.
[35] S.C. Tauber, S. Bunkowski, W. Bruck, R. Nau, Septic metastatic encephalitis: co-existence of brain damage and repair, Neuropathol. Appl. Neurobiol. 37 (7) (2011) 768–776.
[36] T. Sharshar, D. Annane, G.L. de la Grandmaison, J.P. Brouland, N.S. Hopkinson, G. Francoise, The neuropathology of septic shock, Brain Pathol. 14 (1) (2004) 21–33.
[37] M. Deng, R.D. Hofacer, C. Jiang, B. Joseph, E.A. Hughes, B. Jia, S.C. Danzer, A.W. Loepke, Brain regional vulnerability to anaesthesia-induced neuroapoptosis shifts with age at exposure and extends into adulthood for some regions, Br. J. Anaesth. 113 (3) (2014) 443–451.
[38] E. Kolaczkowska, P. Kubes, Neutrophil recruitment and function in health and inflammation, Nat Rev Immunol 13 (3) (2013) 159–175.
[39] A. Greka, B. Navarro, E. Oancea, A. Duggan, D.E. Clapham, TRPC5 is a regulator of hippocampal neurite length and growth cone morphology, Nat. Neurosci. 6 (8) (2003) 837–845.
[40] A. Sumoza-Toledo, R. Penner, TRPM2: a multifunctional ion channel for calcium signalling, J. Physiol. 589 (Pt 7) (2011) 1515–1525.
[41] Y. Hara, M. Wakamori, M. Ishii, E. Maeno, M. Nishida, T. Yoshida, H. Yamada, S. Shimizu, E. Mori, J. Kudoh, N. Shimizu, H. Kurose, Y. Okada, K. Imoto, Y. Mori, LTRPC2 Ca2+−permeable channel activated by changes in redox status confers

susceptibility to cell death, Mol. Cell 9 (1) (2002) 163–173.
[42] A.L. Perraud, A. Fleig, C.A. Dunn, L.A. Bagley, P. Launay, C. Schmitz, A.J. Stokes, Q. Zhu, M.J. Bessman, R. Penner, J.P. Kinet, A.M. Scharenberg, ADP-ribose gating of the calcium-permeable LTRPC2 channel revealed by Nudix motif homology, Nature 411 (6837) (2001) 595–599.
[43] Y. Sano, K. Inamura, A. Miyake, S. Mochizuki, H. Yokoi, H. Matsushime, K. Furuichi, Immunocyte Ca2+ influx system mediated by LTRPC2, Science 293 (5533) (2001) 1327–1330.
[44] E. Wehage, J. Eisfeld, I. Heiner, E. Jungling, C. Zitt, A. Luckhoff, Activation of the cation channel long transient receptor potential channel 2 (LTRPC2) by hydrogen peroxide. A splice variant reveals a mode of activation independent of ADP-ribose, J. Biol. Chem. 277 (26) (2002) 23150–23156.
[45] S. Kaneko, S. Kawakami, Y. Hara, M. Wakamori, E. Itoh, T. Minami, Y. Takada, T. Kume, H. Katsuki, Y. Mori, A. Akaike, A critical role of TRPM2 in neuronal cell death by hydrogen peroxide, J. Pharmacol. Sci. 101 (1) (2006) 66–76.
[46] N.L. Cook, R. Vink, S.C. Helps, J. Manavis, C. van den Heuvel, Transient receptor potential melastatin 2 expression is increased following experimental traumatic brain injury in rats, J. Mol. Neurosci. 42 (2) (2010) 192–199.
[47] J. Wehrhahn, R. Kraft, C. Harteneck, S. Hauschildt, Transient receptor potential melastatin 2 is required for lipopolysaccharide-induced cytokine production in human monocytes, J. Immunol. 184 (5) (2010) 2386–2393.
[48] A.M. Van Dam, H.E. De Vries, J. Kuiper, F.J. Zijlstra, A.G. De Boer, F.J. Tilders, F. Berkenbosch, Interleukin-1 receptors on rat brain endothelial cells: a role in neuroimmune interaction? FASEB J. 10 (2) (1996) 351–356.
[49] E.B. Becker, A. Bonni, Pin1 mediates neural-specific activation of the mitochondrial apoptotic machinery, Neuron 49 (5) (2006) 655–662.
[50] L. Zhang, L. Li, H. Liu, J.L. Borowitz, G.E. Isom, BNIP3 mediates cell death by different pathways following localization to endoplasmic reticulum and mitochondrion, FASEB J. 23 (10) (2009) 3405–3414.
[51] N. Joza, S.A. Susin, E. Daugas, W.L. Stanford, S.K. Cho, C.Y. Li, T. Sasaki, A.J. Elia, H.Y. Cheng, L. Ravagnan, K.F. Ferri, N. Zamzami, A. Wakeham, R. Hakem, H. Yoshida, Y.Y. Kong, T.W. Mak, J.C. Zuniga-Pflucker, G. Kroemer, J.M. Penninger, Essential role of the mitochondrial apoptosis-inducing factor in programmed cell death, Nature 410 (6828) (2001) 549–554.
[52] S.A. Susin, H.K. Lorenzo, N. Zamzami, I. Marzo, B.E. Snow, G.M. Brothers, J. Mangion, E. Jacotot, P. Costantini, M. Loeffler, N. Larochette, D.R. Goodlett, R. Aebersold, D.P. Siderovski, J.M. Penninger, G. Kroemer, Molecular characterization of mitochondrial apoptosis-inducing factor, Nature 397 (6718) (1999) 441–446.
[53] E. Daugas, S.A. Susin, N. Zamzami, K.F. Ferri, T. Irinopoulou, N. Larochette, M.C. Prevost, B. Leber, D. Andrews, J. Penninger, G. Kroemer, Mitochondrio-nuclear translocation of AIF in apoptosis and necrosis, FASEB J. 14 (5) (2000) 729–739.
[54] X. Zhang, J. Chen, S.H. Graham, L. Du, P.M. Kochanek, R. Draviam, F. Guo, P.D. Nathaniel, C. Szabo, S.C. Watkins, R.S. Clark, Intranuclear localization of apoptosis-inducing factor (AIF) and large scale DNA fragmentation after traumatic brain injury in rats and in neuronal cultures exposed to peroxynitrite, J. Neurochem. 82 (1) (2002) 181–191.
[55] E.C. Cheung, L. Melanson-Drapeau, S.P. Cregan, J.L. Vanderluit, K.L. Ferguson, W.C. McIntosh, D.S. Park, S.A. Bennett, R.S. Slack, Apoptosis-inducing factor is a key factor in neuronal cell death propagated by BAX-dependent and BAX-independent mechanisms, J. Neurosci. 25 (6) (2005) 1324–1334.
[56] H.P. Zassenhaus, G. Denniger, Analysis of the role of the NUC1 endo/exonuclease in yeast mitochondrial DNA recombination, Curr. Genet. 25 (2) (1994) 142–149.
[57] M.R. Szymanski, W. Yu, A.M. Gmyrek, M.A. White, I.J. Molineux, J.C. Lee, Y.W. Yin, A domain in human EXOG converts apoptotic endonuclease to DNA-repair exonuclease, Nat. Commun. 8 (2017) 14959.
[58] P.L. Liu, Y.L. Chen, Y.H. Chen, S.J. Lin, Y.R. Kou, Wood smoke extract induces oxidative stress-mediated caspase-independent apoptosis in human lung endothelial cells: role of AIF and EndoG, Am J Physiol Lung Cell Mol Physiol 289 (5) (2005) L739–L749.
[59] J. Parrish, L. Li, K. Klotz, D. Ledwich, X. Wang, D. Xue, Mitochondrial endonuclease G is important for apoptosis in C. elegans, Nature 412 (6842) (2001) 90–94.
[60] X. Wang, C. Yang, J. Chai, Y. Shi, D. Xue, Mechanisms of AIF-mediated apoptotic DNA degradation in Caenorhabditis elegans, Science 298 (5598) (2002) 1587–1592.
[61] G. Liu, H. Zou, T. Luo, M. Long, J. Bian, X. Liu, J. Gu, Y. Yuan, R. Song, Y. Wang, J. Zhu, Z. Liu, Caspase-dependent and caspase-independent pathways are involved in cadmium-induced apoptosis in primary rat proximal tubular cell culture, PLoS One 11 (11) (2016) e0166823.
[62] C.E. Bond, S.A. Greenfield, Multiple cascade effects of oxidative stress on astroglia, Glia 55 (13) (2007) 1348–1361.
[63] S. Watkins, S. Robel, I.F. Kimbrough, S.M. Robert, G. Ellis-Davies, H. Sontheimer, Disruption of astrocyte-vascular coupling and the blood-brain barrier by invading glioma cells, Nat. Commun. 5 (2014) 4196.
[64] C.C. Bowman, A. Rasley, S.L. Tranguch, I. Marriott, Cultured astrocytes express toll-like receptors for bacterial products, Glia 43 (3) (2003) 281–291.
[65] G. Sita, P. Hrelia, A. Graziosi, G. Ravegnini, F. Morroni, TRPM2 in the brain: role in health and disease, Cells 7 (7) (2018).